

# Dimuon and charm production in In+In collisions at the CERN SPS

E. Scomparin for the NA60 Collaboration

R. Arnaldi<sup>10</sup>, R. Averbeck<sup>9</sup>, K. Banicz<sup>2,4</sup>, J. Castor<sup>3</sup>, B. Chaurand<sup>7</sup>, C. Cicalò<sup>1</sup>, A. Colla<sup>10</sup>, P. Cortese<sup>10</sup>, S. Damjanovic<sup>4</sup>, A. David<sup>2,5</sup>, A. De Falco<sup>1</sup>, A. Devaux<sup>3</sup>, A. Drees<sup>9</sup>, L. Ducroux<sup>6</sup>, H. En'yo<sup>8</sup>, A. Ferretti<sup>10</sup>, M. Floris<sup>1</sup>, P. Force<sup>3</sup>, N. Guettet<sup>2,3</sup>, A. Guichard<sup>6</sup>, H. Gulkanian<sup>11</sup>, J. Heuser<sup>8</sup>, M. Keil<sup>2,5</sup>, L. Kluberg<sup>2,7</sup>, C. Lourenço<sup>2</sup>, J. Lozano<sup>5</sup>, F. Manso<sup>3</sup>, A. Masoni<sup>1</sup>, P. Martins<sup>2,5</sup>, A. Neves<sup>5</sup>, H. Ohnishi<sup>8</sup>, C. Oppedisano<sup>10</sup>, P. Parracho<sup>2</sup>, P. Pillot<sup>6</sup>, G. Puddu<sup>1</sup>, E. Radermacher<sup>2</sup>, P. Ramalhete<sup>2</sup>, P. Rosinsky<sup>2</sup>, E. Scomparin<sup>10</sup>, J. Seixas<sup>2,5</sup>, S. Serci<sup>1</sup>, R. Shahoyan<sup>2,5</sup>, P. Sonderegger<sup>5</sup>, H.J. Specht<sup>4</sup>, R. Tieulent<sup>6</sup>, G. Usai<sup>1</sup>, R. Veenhof<sup>2,5</sup>, H.K. Wöhri<sup>2,5</sup>

<sup>1</sup>Univ. di Cagliari and INFN, Cagliari, Italy, <sup>2</sup>CERN, Geneva, Switzerland, <sup>3</sup>LPC, Univ. Blaise Pascal and CNRS-IN2P3, Clermont-Ferrand, France, <sup>4</sup>Univ. Heidelberg, Heidelberg, Germany, <sup>5</sup>IST-CFTP, Lisbon, Portugal, <sup>6</sup>IPN-Lyon, Univ. Claude Bernard Lyon-I and CNRS-IN2P3, Lyon, France, <sup>7</sup>LLR, Ecole Polytechnique and CNRS-IN2P3, Palaiseau, France, <sup>8</sup>RIKEN, Wako, Saitama, Japan, <sup>9</sup>SUNY Stony Brook, New York, USA, <sup>10</sup>Univ. di Torino and INFN, Italy, <sup>11</sup>YerPhI, Yerevan, Armenia

The NA60 experiment studies muon pair production with proton and Indium beams. It is a second generation experiment, designed to answer specific questions left open, in the leptonic sector, by the previous round of SPS experiments, finished in 2000. The results presented in this paper cover the dimuon invariant mass range from the threshold to the  $J/\psi$ . The main physics topics that we address include the in-medium modifications of the  $\rho$  meson, the origin of the dimuon excess observed between the  $\phi$  and the  $J/\psi$ , and the study of the anomalous  $J/\psi$  suppression. For each of these subjects, the NA60 results represent a significant step forward towards a deeper understanding of the physics of heavy ion collisions at SPS energies.

## 1. INTRODUCTION, EXPERIMENTAL SET-UP AND DATA ANALYSIS

Experiments measuring lepton pair production have played an important role in the SPS heavy-ion program since its very beginning, in 1986. The absence of significant re-interactions with the hadronic environment makes dileptons an ideal tool for the study of the early stages of the collision, when thermal dileptons from the deconfined phase should be emitted. Furthermore, vector mesons produced in heavy-ion collisions ( $\rho$ ,  $\omega$ ,  $\phi$ ,  $J/\psi$ ) can be detected in a rather clean way through their decay into lepton pairs.

In the low-mass sector ( $m < m_\phi$ ) the CERES experiment has studied the production of electron pairs in p+Be/Au, S+Au and Pb+Au collisions [1]. In nuclear collisions a clear excess above the expected hadronic sources has been observed. The origin of the excess has been commonly interpreted in terms of thermal production from the dense hadronic

gas created in the collision, mainly occurring via the  $\pi^+\pi^- \rightarrow \rho \rightarrow e^+e^-$  process. Even if it was clear that an in-medium modification of the  $\rho$  must be introduced in order to explain the results, the lack of statistics and mass resolution have prevented any detailed understanding of the character of the in-medium changes.

In the intermediate-mass region, between the  $\phi$  and the  $J/\psi$ , the HELIOS-3 [2] and the NA38/NA50 [3] experiments have discovered in S+W/U and Pb+Pb collisions an excess in the dimuon yield over the expected sources, the Drell-Yan process (DY) and the semi-leptonic decay of charmed meson pairs ( $D\bar{D}$ ). Such an excess smoothly increases as a function of centrality, up to the most central Pb+Pb collisions. However, mainly because of the lack of experimental capability in distinguishing ‘prompt’ dimuon production from open charm decay muons, the origin of the excess has remained unexplained until now.

Finally, the NA50 experiment has discovered the so-called anomalous  $J/\psi$  suppression, considered as one of the ‘smoking guns’ for the observation of deconfinement at SPS energies. It was observed that the onset of the suppression occurs within a relatively narrow centrality interval, suggesting a kind of threshold behavior. However, it is not clear up to now which is the physics variable at the basis of the anomalous suppression, candidates being the energy density, for thermal models of the  $J/\psi$  melting, or the density of participants, in the framework of percolation approaches.

The importance of these observations, as well as the need to better clarify them, has lead to the proposal and approval of a second generation experiment, NA60. With respect to previous experiments, NA60 has strongly improved the dilepton detection techniques. In terms of detector layout, the experiment is based on the muon spectrometer and zero-degree calorimeter inherited from NA50. However, the vertex region has been completely re-designed, including now a vertex telescope (VT), made of silicon pixel planes embedded in a 2.5 T dipole magnetic field, and a Beam Tracker (BT), measuring the transverse position of the incident ion before its interaction in the target (see Fig. 1 for the layout of vertex region of the apparatus).

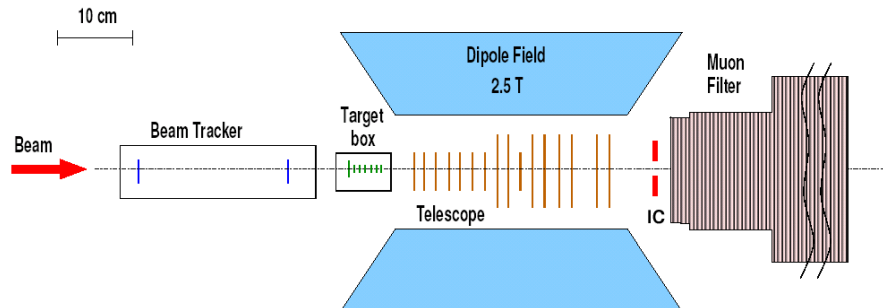


Figure 1. Layout of the vertex region of the NA60 experiment.

Thanks to the vertex detectors, the primary interaction vertex can now be determined with an accuracy of the order of 10–15  $\mu\text{m}$  in the transverse plane and  $\sim 200 \mu\text{m}$  along the beam axis. By matching the muons measured in the muon spectrometer to tracks in the vertex telescope, using information on coordinates and momentum simultaneously,

it is possible to overcome the uncertainties introduced by multiple scattering and energy loss fluctuations, due to the crossing of the hadron absorber. In this way, a very good invariant mass resolution has been achieved ( $\sim 20$  MeV at the  $\omega$ ). Finally, it is possible to measure the offset of the muon with respect to the interaction vertex. This is done with a resolution of  $\sim 50$   $\mu\text{m}$  in the transverse plane. In this way we separate prompt dimuons (DY, thermal) from muon pairs due to D-meson decays.

The experiment has taken data in 2003 (In+In collisions) and 2004 (p+A). The results shown in this paper refer to the five-week long 2003 run. In this period, about  $4 \cdot 10^{12}$  Indium ions, with an energy of 158 GeV/nucleon, have been delivered and more than 200 million dimuon events have been collected. Two muon spectrometer settings have been used in the data taking. The first one (set A) corresponds to a relatively low magnetic field in the muon spectrometer magnet, leading to an enhancement of the acceptance of the setup for low-mass dimuons; the corresponding data have been used for the low and intermediate-mass analysis. The second data sample (set B) has been taken with a higher magnetic field, in order to reduce the deadtime of the data acquisition and improve the mass resolution at the  $J/\psi$ , and has been used for the study of high-mass dimuons. The centrality selection can be performed either by using the zero-degree energy, directly correlated with the number of projectile spectators, or the charged particle multiplicity, as measured in the vertex spectrometer acceptance ( $3 < \eta < 4$ ).

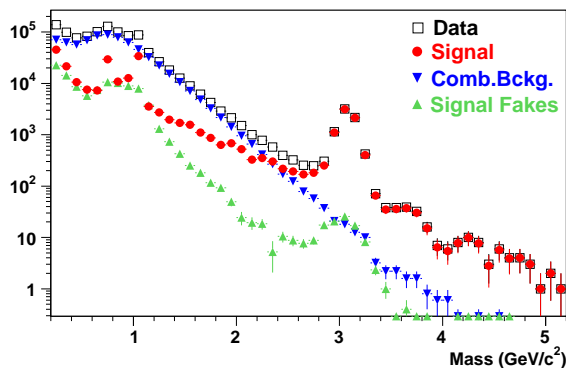


Figure 2. Opposite-sign dimuon data, combinatorial background (CB), fake signal and final correctly matched signal.

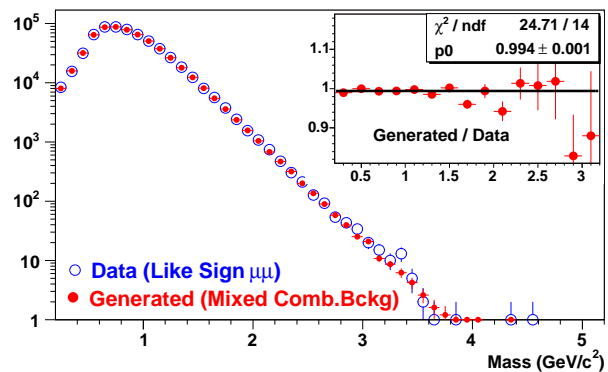


Figure 3. Measured and generated like-sign CB spectra. The insert shows the ratio between mixed and measured distributions.

In Fig. 2 (open squares) we show the opposite-sign dimuon mass spectrum corresponding to set A. Two kinds of background affect the NA60 data. The first one is the usual combinatorial background, due to uncorrelated  $\pi$  and K decays. This background has been subtracted by means of a mixed-event technique. Opposite-sign muon pairs are created combining single muons from different like-sign events, respecting the acceptance and trigger conditions of the spectrometer. The procedure has been tested by comparing the measured like-sign mass distribution with the corresponding one generated with the mixed-event algorithm (see Fig. 3). An agreement within 1% is found. Since the signal to background ratio is of the order of  $1/10$ , the systematic error on the signal extraction

is therefore of the order of 10%. Another source of background originates when a muon track measured in the muon spectrometer is matched to a wrong vertex spectrometer track. This ‘fake matches’ background can also be subtracted by means of a mixed-event procedure, or with an overlay Monte-Carlo method (see [5]). The two techniques agree to within 5%, a number representing a realistic systematic uncertainty on this evaluation. The contribution of fake matches to the measured signal is much smaller than the combinatorial background, as can be seen in Fig. 2. It reaches a maximum in the low-mass continuum where it is, at most, of the same order of magnitude as the signal.

## 2. THE LOW-MASS REGION

This analysis [7] has been carried out on the spectrum shown in Fig. 4, containing about 360 000 signal pairs. For the first time in nuclear collisions, clear  $\omega$  and  $\phi$  signals have been detected, and even the helicity-suppressed  $\eta \rightarrow \mu\mu$  decay is visible in our spectrum. Data analysis has been performed in four centrality bins, defined through the charged particle multiplicity  $dN_{\text{ch}}/d\eta$  in the vertex spectrometer.

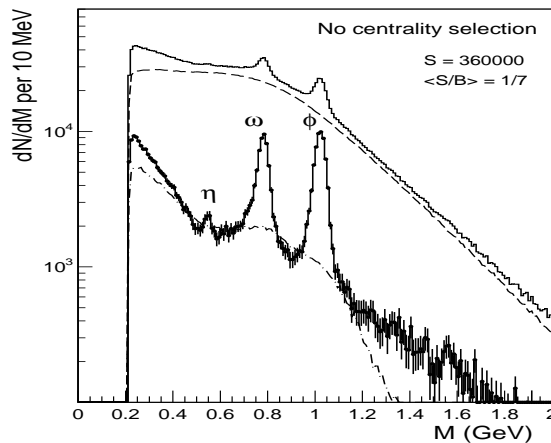


Figure 4. Dimuon mass spectra for opposite-sign pairs (upper histogram), combinatorial background (dashed), fake matches (dashed-dotted), and final signal.

The most peripheral data ( $4 < dN_{\text{ch}}/d\eta < 30$ ) have been described on the basis of known sources, i.e. the two-muon decays of  $\eta$ ,  $\rho$ ,  $\omega$  and  $\phi$ , plus the Dalitz decays of  $\eta$ ,  $\eta'$  and  $\omega$ , and a contribution from open charm decays. This ‘hadronic’ cocktail has been directly fitted to the data and, as can be seen in Fig. 5, is found to reproduce quite well the observed spectrum. The free parameters in the fit are the cross-section ratios  $\eta/\omega$ ,  $\rho/\omega$ ,  $\phi/\omega$ , the open charm yield and an overall normalization factor. The expected mass shape for the various physics processes has been obtained propagating decay muons through the NA60 set-up, using GENESIS as event generator and GEANT for tracking. In Fig. 6 we show the values of the meson cross-section ratios, as obtained from the fit of our peripheral data, in several  $p_{\text{T}}$  bins. It can be seen that the  $\eta/\omega$  values nicely agree with the world average for p+p and p+Be, while the  $\phi/\omega$  ratio is higher, as to be expected from the previous observations [6] of the  $\phi$  enhancement in nuclear collisions.

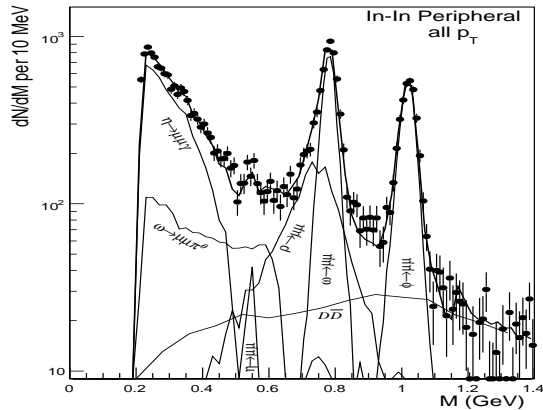


Figure 5. Fit of the peripheral In+In low-mass region. See text for details.

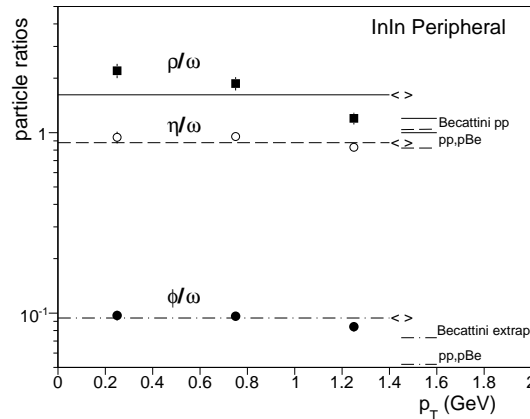


Figure 6. Meson cross-section ratios, as extracted from the fit, in three  $p_T$  bins, for the peripheral centrality class.

Finally, the observed increase of the  $\rho/\omega$  ratio at low  $p_T$  indicates some contribution from  $\pi\pi$  annihilation already in peripheral In+In collisions. Moving to more central collisions, the fit procedure is no longer satisfactory, due to the presence of a strong excess with a priori unknown characteristics. Therefore, we have rather ‘subtracted’ the hadronic cocktail contributions (except for the  $\rho$ ) from the data. The  $\omega$  and  $\phi$  yields have been fixed so that, after subtraction, a smooth underlying continuum is obtained. The  $\eta$  yield has been fixed by imposing that in the mass region close to threshold the dimuon yield is entirely due to the Dalitz-decay of this meson, thereby locally minimizing the possible excess. For more details see [7].

As a result we see that the excess mass spectra exhibit, for all centrality bins, a resonance-like structure, centered at the nominal position of the  $\rho$  pole, but strongly broadened (see Fig. 7, where the result for the most central bin is shown). With respect to the expected  $\rho$  yield, the excess increases with centrality, reaching a factor  $>4$  for central events. For such events, the size of the systematic error on the excess evaluation, due to the systematic uncertainty on the background subtraction, is of the order of 25%, while it is significantly lower for peripheral events. Finally, in Fig. 8 we compare our excess mass distribution with theoretical calculations that predict either an in-medium broadening of the  $\rho$  (Rapp-Wambach [8], solid thick line), or a shift of the  $\rho$  pole (related to Brown-Rho scaling [9], dashed-dotted line). The result clearly indicates that a significant shift of the  $\rho$  mass is ruled out, while the broadening scenario appears more realistic.

$\phi$  meson production has been studied as a function of centrality, with a particular emphasis on the  $p_T$  distributions [10]. A long-standing puzzle on this topic exists at SPS energy. Experiments NA49 (in the  $\phi \rightarrow KK$  decay mode) and NA50 (in the  $\phi \rightarrow \mu\mu$  decay mode) measured different behaviors in the transverse momentum distributions, parameterized through the inverse slope parameter,  $T$ . In particular, NA49 [11] has observed a significantly higher  $T$  parameter, increasing with centrality, while NA50 [6] showed no dependence of  $T$  on centrality. NA60 can cleanly measure the  $\phi \rightarrow \mu\mu$  decay

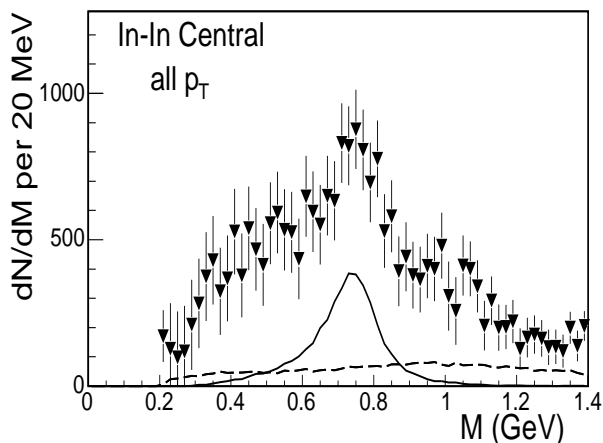


Figure 7. Excess mass spectra for the most central bin: the cocktail  $\rho$  (solid line) and the contribution from open charm decays (dashed) are also shown.

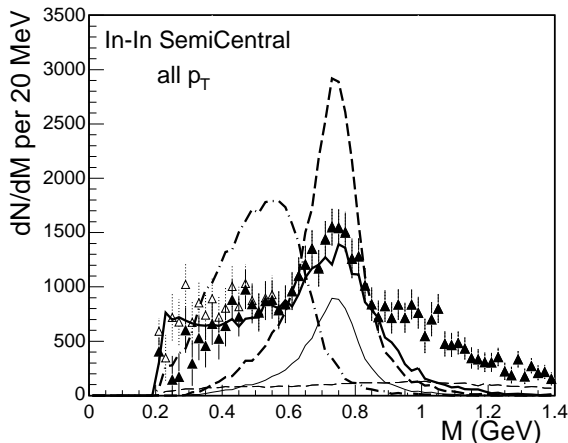


Figure 8. Comparison of the excess with model predictions. The open triangles correspond to lowering the  $\eta$  yield by 10%. See the text for further details.

and can in principle access the  $\phi \rightarrow KK$  channel by combining all the tracks reconstructed in the vertex telescope (no particle identification can be performed). For the time being, results are available in the dimuon channel and are shown in Fig. 9, as a function of  $N_{\text{part}}$ , together with previous results. The  $T$  parameter increases with centrality, in agreement with the NA49 data. The NA60 In-In value integrated over all centralities is  $T = 253 \pm 2$  MeV, and lies between the Si+Si and Pb+Pb values measured by NA49 ( $\sim 220$  and  $290$  MeV, respectively), as expected, while the NA50 Pb-Pb point ( $T \approx 228$  MeV) is lower than expected from the general trend of the  $T$  parameter as a function of the mass. From these considerations we conclude that the NA60 measurement seems to agree with the NA49 values, so that the difference between the NA49 and NA50 measurements cannot be attributed to the different decay channels probed.

### 3. THE INTERMEDIATE-MASS REGION

The excess observed by previous experiments between the  $\phi$  and the  $J/\psi$  could be interpreted in terms of an anomalous open charm enhancement in nuclear collisions, or as being due to the production of thermal dimuons. This conclusion was essentially based on the analysis of the dimuon mass and transverse momentum distributions, not involving any identification of the open charm decay vertex. As a first step, NA60 has also performed such an analysis. Drell-Yan and open charm contributions were generated with Pythia 6.2 using CTEQ6M PDFs with EKS98 nuclear modifications, and tracked through our setup using GEANT. The Drell-Yan normalization has been fixed so as to reproduce the high-mass cross section measured by NA50, while for open charm the value  $\sigma_{c\bar{c}} = 12 \mu\text{b/nucleon}$  has been taken, again in order to reproduce the NA50 analysis of the 450 GeV p+A data [3]. It must be noted that such an open charm cross section is

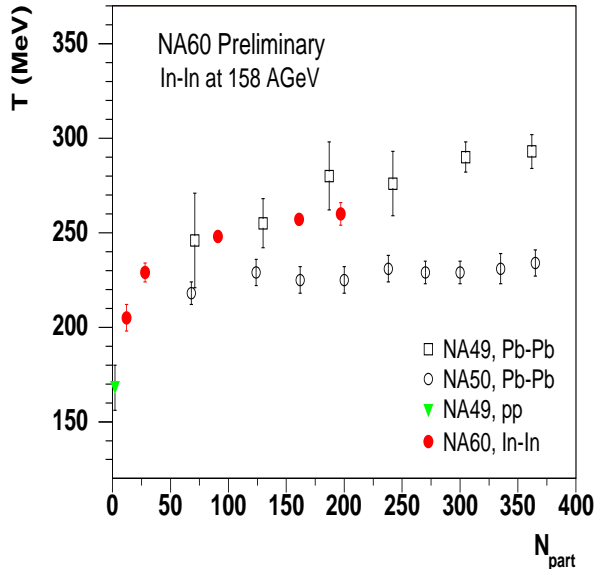


Figure 9. Inverse slope  $T$  as a function of the number of participants, as measured by NA60, NA49 and NA50.

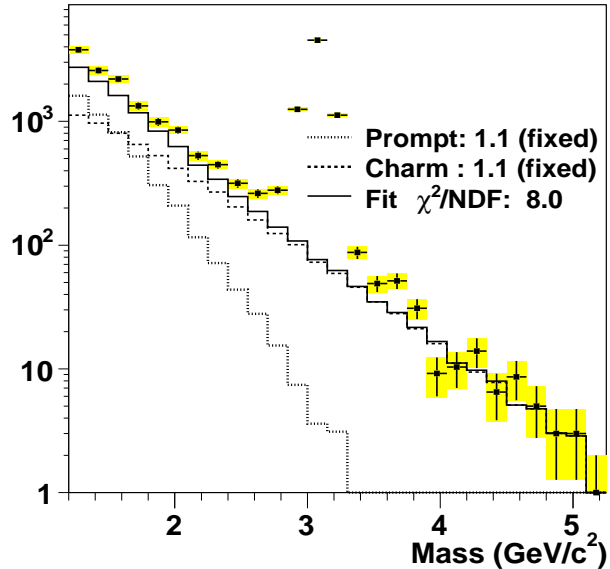


Figure 10. Fit of IMR mass spectrum to the superposition of the expected Drell-Yan and open charm contributions.

about twice higher than the world average at this energy. The data are analyzed in the kinematic domain  $0 < y_{CM} < 1$ ,  $|\cos \theta_{CS}| < 0.5$  and  $1.2 < m_{\mu\mu} < 2.7$ . In Fig. 10 we show a comparison of the expected sources with the measured signal spectrum. A clear excess can be seen, thereby confirming the observations of the previous experiments.

Thanks to the excellent vertex capabilities, NA60 can go a step forward and tag open charm decays through the measurement of the offset of the muon with respect to the position of the primary vertex. In practice, we build, for the intermediate mass dimuons, a distribution of the weighted offsets (see [5] for details of the weighting procedure). This distribution is then fitted to a superposition of the expected weighted offset distributions for prompt and open charm dimuons. For the former, the shape of the sum of the measured  $J/\psi$  and  $\phi$  offsets is used, while for charm we use the Monte-Carlo shape, smeared to account for the difference between the Monte-Carlo and data observed in the  $J/\psi$  and  $\phi$  signals. Fig. 11 shows the result of the fit with the prompt contribution normalized to the expected Drell-Yan and the open charm left free. The latter is too flat to describe the data. Letting both contributions vary freely, as shown in Fig. 12, gives a good description of the data, with an open charm contribution compatible with the expected one, but with a prompt contribution almost two times higher than the expected Drell-Yan. Therefore, the excess measured by NA60 is compatible with a prompt source. A preliminary analysis of the centrality dependence of the excess [5] shows that it rises faster than linearly with the number of participants.

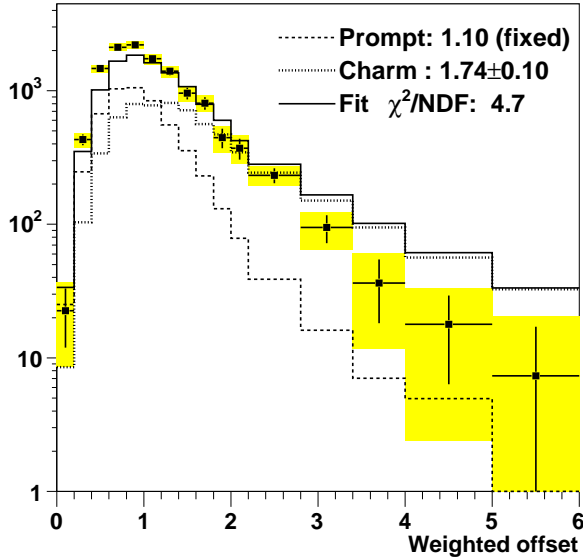


Figure 11. Fit of IMR dimuon weighted offset spectrum, with the open charm contribution as a free parameter.

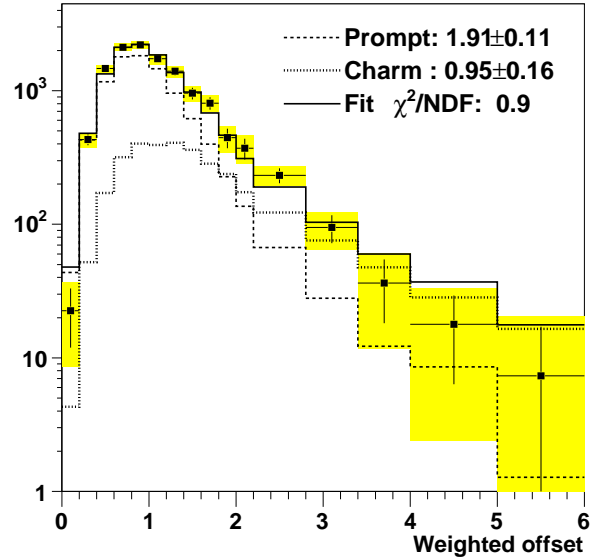


Figure 12. Fit of IMR dimuon weighted offset spectrum, with the open charm and prompt contributions free.

#### 4. THE HIGH-MASS REGION

In Pb+Pb collisions, above a certain centrality threshold, an anomalous  $J/\psi$  suppression has been seen by NA50, i.e. suppression mechanisms different from nuclear absorption must be invoked to explain the observed  $J/\psi$  yield. However, several questions raised by this observation have still to be clarified. By studying  $J/\psi$  production in In+In collisions, NA60 wants to investigate the onset of the anomalous  $J/\psi$  behaviour in systems lighter than Pb+Pb, and use this result to study which is the physics variable, related to centrality, that drives  $J/\psi$  suppression.

Two different analyses have been performed by NA60 [12] to investigate the centrality dependence of the  $J/\psi$  production, corresponding to two different ways of normalizing its yield. The first technique, the so-called ‘standard analysis’, is based on a normalization to the Drell-Yan events, already widely used in the past by NA38/NA50. The study of the ratio between the  $J/\psi$  and the Drell-Yan cross sections has the advantage of being free from systematic errors connected with the efficiency and luminosity evaluations. However, the statistical error is large, due to the small number of high-mass Drell-Yan pairs (a few hundreds); therefore no more than three centrality bins, defined through the zero-degree energy, can be defined. The second technique overcomes the statistical problem, directly studying the measured  $J/\psi$  centrality distribution, plotted as a function of  $E_{ZDC}$  and corrected by the small inefficiencies due to the reconstruction procedure and the event selection. This distribution is then compared with the expected pattern in case nuclear absorption would be the only active suppression mechanism. This reference curve is obtained with the Glauber model, assuming that  $J/\psi$  production is a hard process, and using  $\sigma_{abs}=4.18$  mb for the nuclear absorption cross section of the  $c\bar{c}$  pair [13]. In such an

analysis, the relative normalization between data and the reference curve is not fixed a priori. We have therefore imposed the centrality-averaged ratio between data and reference to be equal to the one obtained in the standard analysis. Since the average  $\sigma_{J/\psi}/\sigma_{DY}$  ratio has been measured with a 7% statistical error, such an overall error (not shown in the figures) applies to the results. In Fig. 13 we show, as a function of  $E_{ZDC}$  and for both

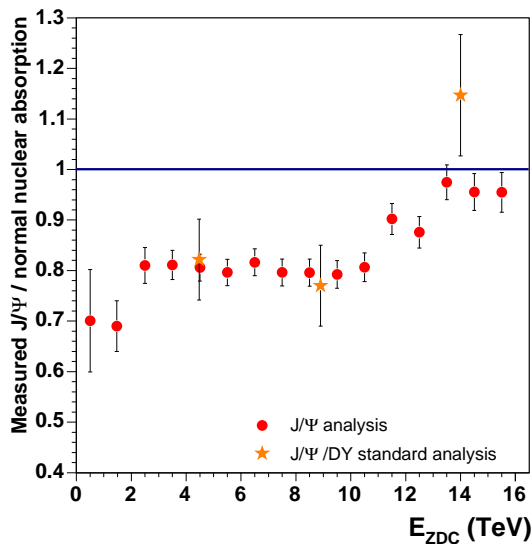


Figure 13. The measured/expected  $J/\psi$  yield as a function of  $E_{ZDC}$ .

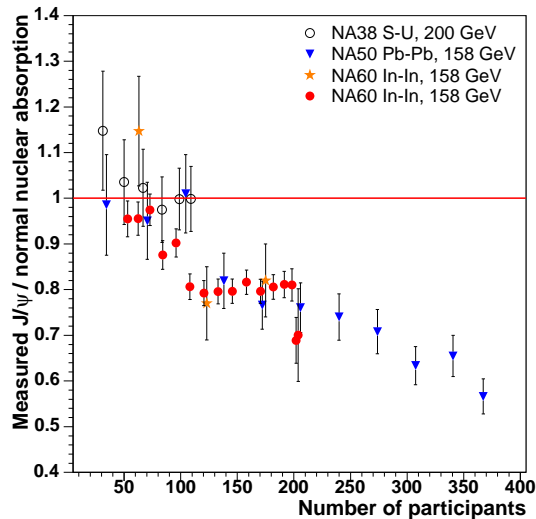


Figure 14.  $J/\psi$  suppression pattern measured in S+U, In+In and Pb+Pb, as a function of  $N_{part}$ .

analysis, the ratio between the measured and expected  $J/\psi$  yields. While the peripheral points are compatible with the nuclear absorption scenario, an anomalous suppression sets in at  $E_{ZDC} \sim 12$  TeV. In Fig. 14 the  $J/\psi$  suppression pattern measured in In+In collisions is compared with the results obtained for S+U and Pb+Pb by NA38/NA50, using  $N_{part}$  as centrality estimator. Even if  $N_{part}$  seems to be a reasonable scaling variable for the anomalous suppression, it is fair to say that more accurate data for the previously studied collision systems are needed in order to establish a firm conclusion on the variable driving the suppression mechanism. For comparisons as a function of other centrality related variables see [12]. Finally, a few theoretical predictions for  $J/\psi$  suppression in In+In exist, based either on the interaction with comovers [14], on a percolation scenario [15] or, finally, on dissociation and regeneration of the  $J/\psi$  in both QGP and hadronic phases [16]. They are compared to our data in Fig. 15. It can be seen that none of them is able to reproduce our results over the whole centrality range.

## 5. CONCLUSIONS

The NA60 experiment measured muon pair production in In+In collisions at 158 GeV per nucleon. Preliminary results are now available for the main topics at the basis of the

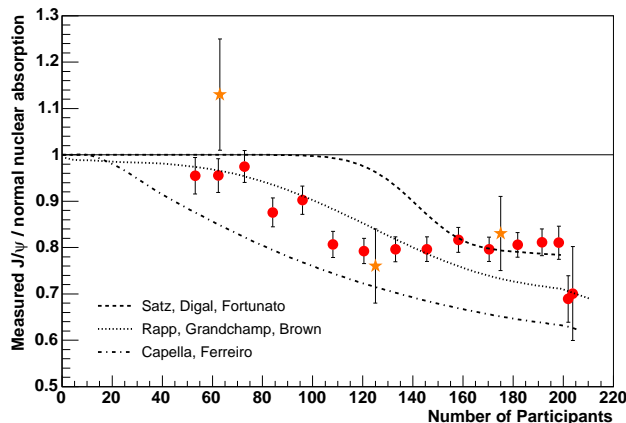


Figure 15. Comparison of the In+In suppression pattern with theoretical predictions.

physics program of the experiment. In the low mass region, we find an excess with respect to the expected sources, increasing with centrality. The qualitative features of the excess spectra are consistent with an interpretation in terms of  $\pi\pi$  annihilation. Even for central collisions the  $\rho$  does not show any noticeable shift in mass. Concerning the  $\phi$  meson, the inverse slope parameter  $T$  extracted from the  $p_T$  spectra increases with centrality, in agreement with previous observations by NA49. In the intermediate mass region, the dimuon excess observed by Helios-3 and NA38/NA50 has been confirmed and we show that it is due to a prompt source rather than to an enhancement of the open charm yield. Finally, an anomalous  $J/\psi$  suppression has been observed also in In+In collisions. It sets in at  $N_{\text{part}} \sim 90$ , in qualitative agreement with previous observations carried out in Pb+Pb.

## REFERENCES

1. G. Agakichiev et al. (CERES Coll.), Eur. Phys. J. C41 (2005) 475.
2. A.L.S. Angelis et al. (HELIOS-3 Coll.), Eur. Phys. J. C13 (2000) 433.
3. M.C. Abreu et al. (NA38/NA50 Coll.), Eur. Phys. J. C14 (2000) 443.
4. M.C. Abreu et al. (NA50 Coll.), Eur. Phys. J. C39 (2005) 335.
5. R. Shahoyan et al. (NA60 Coll.), these proceedings, and references therein.
6. B. Alessandro et al. (NA50 coll.), Phys. Lett. B 555 (2003) 147.
7. S. Damjanovic et al. (NA60 Coll.), these proceedings, and references therein.
8. R. Rapp and J. Wambach, Adv.Nucl.Phys. 25 (2000) 1.
9. G.E. Brown and M. Rho, Phys.Rept. 363 (2002) 85.
10. A. De Falco et al. (NA60 Coll.), these proceedings, and references therein.
11. S.V. Afanasiev et al. (NA49 coll.), Phys. Lett. B 491 (2000) 59.
12. R. Arnaldi et al. (NA60 Coll.), these proceedings, and references therein.
13. G. Borges et al. (NA50 Coll.), Eur. Phys. J. C43 (2005) 161.
14. A. Capella and E. Ferreiro, hep-ph/0505032.
15. S. Digal, S. Fortunato and H. Satz, Eur. Phys. J. C32 (2004) 547.
16. L. Grandchamp, R. Rapp and G. Brown, J. Phys. G30 (2004) S1355.